

UC Irvine

UC Irvine Previously Published Works

Title

Monoglyceride lipase: Structure and inhibitors

Permalink

<https://escholarship.org/uc/item/5q94j0t4>

Journal

Chemistry and Physics of Lipids, 197

ISSN

0009-3084

Authors

Scalvini, Laura

Piomelli, Daniele

Mor, Marco

Publication Date

2016-05-01

DOI

10.1016/j.chemphyslip.2015.07.011

Copyright Information

This work is made available under the terms of a Creative Commons Attribution License, available at <https://creativecommons.org/licenses/by/4.0/>

Peer reviewed



HHS Public Access

Author manuscript

Chem Phys Lipids. Author manuscript; available in PMC 2017 May 01.

Published in final edited form as:

Chem Phys Lipids. 2016 May ; 197: 13–24. doi:10.1016/j.chemphyslip.2015.07.011.

Monoglyceride lipase: structure and inhibitors

Laura Scalvini^a, Daniele Piomelli^{b,c,d}, and Marco Mor^a

^aDipartimento di Farmacia, Università degli Studi di Parma, I-43124, Parma, Italy

^bDepartment of Anatomy and Neurobiology, University of California, Irvine, Irvine, CA 92697

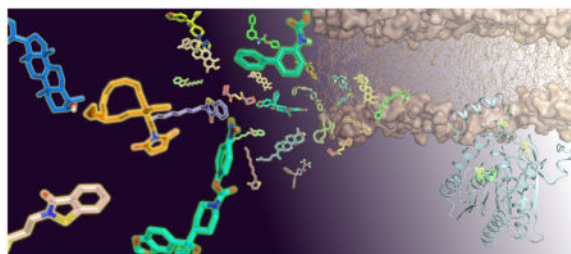
^cDepartment of Biological Chemistry, University of California, Irvine, Irvine, CA 92697

^dUnit of Drug Discovery and Development, Istituto Italiano di Tecnologia, Genova, Italy

Abstract

Monoglyceride lipase (MGL), the main enzyme responsible for the hydrolytic deactivation of the endocannabinoid 2-arachidonoyl-*sn*-glycerol (2-AG), is an intracellular serine hydrolase that plays critical roles in many physiological and pathological processes, such as pain, inflammation, neuroprotection and cancer. The crystal structures of MGL that are currently available provide valuable information about how this enzyme might function and interact with site-directed small-molecule inhibitors. On the other hand, its conformational equilibria and the contribution of regulatory cysteine residues present within the substrate-binding pocket or on protein surface remain open issues. Several classes of MGL inhibitors have been developed, from early reversible ones, such as URB602 and pristimerin, to carbamoylating agents that react with the catalytic serine, such as JZL184 and more recent O-hexafluoroisopropyl carbamates. Other inhibitors that modulate MGL activity by interacting with conserved regulatory cysteines act through mechanisms that deserve to be more thoroughly investigated.

Graphical Abstract



*Corresponding Authors: Dr. Marco Mor, Dipartimento di Farmacia, Università degli Studi di Parma, Parco Area delle Scienze 27/A, I-43124, Parma, Italy, marco.mor@unipr.it. Dr. Daniele Piomelli, Department of Anatomy and Neurobiology, 3216 Gillespie NRF, University of California, Irvine, CA 92697-4625. piomelli@uci.edu.

Publisher's Disclaimer: This is a PDF file of an unedited manuscript that has been accepted for publication. As a service to our customers we are providing this early version of the manuscript. The manuscript will undergo copyediting, typesetting, and review of the resulting proof before it is published in its final citable form. Please note that during the production process errors may be discovered which could affect the content, and all legal disclaimers that apply to the journal pertain.

Keywords

Monoglyceride lipase (MGL); 2-arachidonoyl-*sn*-glycerol (2-AG); endocannabinoids; lid domain; cysteines; inhibitors

1. Introduction

Shortly after the discovery of anandamide in 1992 (Devane et al. 1992), a second endogenous ligand for cannabinoid receptors, 2-arachidonoyl-*sn*-glycerol (2-AG), was identified and quickly recognized as a primary component of endocannabinoid neurotransmission in the central nervous system (CNS) (Mechoulam et al., 1995; Sugiura et al., 1995; Stella et al., 1997). Anandamide and 2-AG activate two G protein-coupled receptors, CB₁ and CB₂ cannabinoid receptors, which are found throughout the mammalian body, but are particularly abundant in the brain (CB₁) and immune cells (CB₂). The endocannabinoids are produced through stimulus-dependent cleavage of membrane phospholipid precursors and are rapidly degraded after their release into the extracellular space. Their on-demand production, their actions explicated near the site of biosynthesis and their rapid deactivation make the endocannabinoids particularly well-suited to mediate short-range neural cellular communication. For example, it has been shown that 2-AG plays a key role in synaptic plasticity and acts as a modulator of neurotransmitter release and neuronal network activity involved in cognition and nociception, among other functions (Hájos et al., 2000; Izumi and Zorumski, 2012; Higgins et al., 2013). Furthermore, 2-AG-dependent short-range modulation has also been implicated in the development of neurons from neural progenitor cells (Aguado et al., 2005; Aguado et al., 2006; Oudin et al., 2011; Gomez et al., 2010; for review, see Galve-Roperh et al., 2013). Similarly, anandamide is responsible for the control of stress-dependent synaptic plasticity in the amygdala (Puente et al., 2011), for the modulation of stress responses and anxiety (Kathuria et al., 2003; Bortolato et al., 2007) and contributes to the control of nociceptive transmission (Clapper et al., 2007; Clapper et al., 2010).

2. An overview of the endocannabinoid system

2.1. Endocannabinoid biosynthesis

Although anandamide and 2-AG share several chemical and functional properties, they are different in the mechanisms underlying their biosynthesis and the cellular events leading to their deactivation. Three pathways have been identified as responsible for anandamide mobilization (for recent reviews see Ueda et al., 2013 and Piomelli, 2014). An *N*-acyltransferase/phospholipase D-dependent pathway mediates the canonical biosynthetic pathway for anandamide (Di Marzo et al. 1994). On the other hand, the route involved in 2-AG production starts from the precursor phosphatidylinositol-4,5-bisphosphate and proceeds through reactions catalyzed by phospholipase C and diacylglycerol lipase (DGL) (Stella et al., 1997; Bisogno et al., 2003; Piomelli et al., 2007).

2.2. Endocannabinoid degradation

Both anandamide and 2-AG are deactivated through a two-steps mechanism, consisting of a selective carrier-based uptake into cells followed by enzymatic hydrolysis. In the CNS, anandamide is hydrolyzed by fatty acid amide hydrolase (FAAH), an amidase-signature enzyme. FAAH hydrolyzes with different efficiencies anandamide, non-cannabinoid fatty acyl ethanolamides such as palmitoylethanolamide (PEA), and also fatty acyl esters, including 2-AG, at least *in vitro*. This apparent promiscuity had led to hypothesize that FAAH might be involved in the hydrolysis of both anandamide and 2-AG; however, this idea has been definitely ruled out by the data. For example, Beltramo and Piomelli found that BTNP ((*E*)-6-(bromo-methylene)-tetrahydro-3-(naphthalen-1-yl)-2*H*-pyran-2-one), an inhibitor of FAAH, does not affect 2-AG hydrolysis at concentrations that block anandamide degradation (Beltramo and Piomelli, 2000). More stringently, Lichtman and coworkers showed that 2-AG hydrolysis is maintained in mutant FAAH^{-/-} mice, and that 2-AG-mediated effects are similar in FAAH^{+/+} and FAAH^{-/-} mice, clearly indicating that an enzyme different from FAAH is responsible for the degradation of 2-AG *in vivo* (Lichtman et al., 2002).

2.3. MGL is the main 2-AG-degrading enzyme

Dinh and coworkers showed that MGL, a serine hydrolase that cleaves 2- and 1-monoglycerides into fatty acids and glycerol (Karlsson et al., 1997), hydrolyzes 2-AG in intact cells (Dinh et al. 2002a). These authors used adenovirus-mediated gene transfer to investigate the role of MGL in 2-AG degradation in brain cortical neurons, and found that MGL overexpression is correlated to attenuation of NMDA/carbachol-induced accumulation of 2-AG, while not affecting 2-AG biosynthesis or anandamide levels. Subsequent experiments using RNAi-mediated silencing (Dinh et al., 2004) and, eventually, deletion by homologous recombination of the *mgl1* gene encoding for MGL (Schlosburg et al., 2010), confirmed that MGL plays a key role in the physiological degradation of 2-AG. Dinh and coworkers also determined the anatomical distribution of the enzyme, showing that, in contrast to FAAH, which is broadly distributed in the CNS, MGL is found in discrete areas, including the hippocampus, the cerebellum, the anterodorsal nucleus of thalamus and the cortex (Dinh et al., 2002b). Interestingly, those areas are also characterized by high expression of CB₁ cannabinoid receptors (Hajos et al., 2000), which is consistent with the role of MGL in terminating the cannabinergic effects of endogenously produced 2-AG near its site of action (Figure 1). A more detailed characterization of the anatomic distribution of MGL and FAAH showed that the expression of both enzymes matches that of CB₁ receptor, but also that the distribution of MGL is complementary to that of FAAH, and that the two enzymes are situated in distinct neuronal compartments (Gulyas et al., 2004; Dinh et al., 2002b). Immunolabeling experiments localized MGL, similarly to CB₁, to presynaptic nerve terminals of glutamatergic neurons, where the enzyme may contribute to terminate the modulatory effects of 2-AG on excitatory transmission. The presence of MGL in other neuronal subpopulations, including CCK-positive GABA-ergic interneurons, suggests that the lipase may be involved in stopping the effects of 2-AG also in this neuronal population. On the other hand, while the distribution of FAAH overlaps that of CB₁ and MGL at a regional level, its expression is mainly postsynaptic (Dinh et al., 2002b). It is important to

point out that the biological functions of MGL are not limited to the deactivation of 2-AG. In addition to mediating the release of fatty acid from monoacylglycerols in adipose tissue (Tornqvist and Belfrage, 1976; Karlsson et al., 1997), MGL also contributes in important ways to the generation of non-esterified arachidonic acid for eicosanoid biosynthesis in a variety of cell types (Bell et al., 1979; Bell et al., 1980; Nomura et al., 2011). A role for this enzyme in the control of multiple lipid modulators in cancer cells has also been postulated (Nomura et al., 2010).

While pharmacological and genetic experiments have documented the fundamental role of MGL in 2-AG degradation, there is also evidence for an MGL-independent route of 2-AG hydrolysis (Muccioli et al., 2007). A functional proteomic approach revealed that, in addition to MGL, two other serine hydrolase might participate in 2-AG hydrolysis in mouse brain membranes (Blankman et al., 2007). These enzymes, α - β hydrolase domain ABHD-12 and ABHD-6 (Figure 1), account for $\approx 9\%$ and $\approx 4\%$, respectively, of total 2-AG hydrolysis in vitro. Subsequent work has confirmed a role for ABHD-6, which is localized postsynaptically, in 2-AG-mediated endocannabinoid transmission (Marrs et al., 2010), whereas ABHD-12 is likely to catalyze the hydrolysis of other lipid substances (Blankman et al., 2013).

Beside MGL and ABHD-6, cyclooxygenase-2 (COX2) has also emerged as a modulator of endocannabinoid levels (Kim and Alger, 2007; Jhaveri et al., 2008; Hermanson et al., 2014), including those of 2-AG (Kozak et al., 2000; Kozak et al., 2001). COX2 oxidizes 2-AG, as well as arachidonic acid and anandamide, giving rise to multiple biologically active modulators. These include prostaglandin E₂ glycerol ester (PGE₂-G, Hu et al., 2008) and prostaglandins, which promote neural inflammation (Nomura et al., 2011; Valdeolivas et al., 2013). These data broaden the biological scope of endocannabinoid signaling, which appears to be, from a general point of view, a crossroad between a diversity of physiological processes.

3. Structure of MGL

3.1. Characterization of MGL

Since MGL was first purified from rat adipose tissue in 1976 (Tornqvist and Belfrage, 1976), a great deal of effort has gone into the characterization of the structure and function of this enzyme.

Rat, mouse and human MGL consist of 303 amino acids, with 84.2% and 83.8%, respectively, of sequence identity for both rMGL and mMGL with hMGL and 92% identity between rMGL and mMGL. Karlsson and coworkers cloned MGL from a mouse adipocyte cDNA library (Karlsson et al., 1997), and identified by site-directed mutagenesis its highly conserved catalytic triad, consisting of residues Ser122, Asp239 and His269. Rat brain MGL was cloned in 2002 (Dinh et al., 2002) and further characterized in 2005 (Saario et al., 2005). These results, and those obtained from the mass-spectrometry characterization of human MGL (Zvonok et al., 2008a; Zvonok et al., 2008b), have helped to elucidate the basic mechanism through which MGL catalyzes the hydrolysis of 2-AG and other monoacylglycerols.

Beside the characterization of the catalytic triad, results showing that MGL is sensitive to inhibition by *p*-chloromercuribenzoic acid (*p*CMB), mercury chloride (HgCl₂) and *N*-ethylmaleimide (Tornqvist and Belfrage, 1976) led to the conclusion that MGL contains at least one sulfhydryl-sensitive site that is needed for enzymatic activity (Saario et al., 2005). In an attempt to characterize the functional role of cysteine residues and predict their localization, Saario and coworkers built a homology model of rat MGL. They identified Cys208 and Cys242 near the catalytic site, and tested a series of maleimide-based compounds for their ability to inhibit MGL activity, providing evidence for irreversible enzyme inhibition mediated by covalent modification of these two residues. More recently, mass spectrometry studies have shown that *N*-arachidonoylmaleimide forms a Michael adduct with Cys242 (Zvonok et al., 2008b). Following this finding, other groups have attempted to characterize the role played by cysteine residues in regulating the enzymatic activity of MGL. Labar and coworkers hypothesized a reversible mechanism to explain the ability of disulfiram (tetraethylthiuram disulphide) to inhibit MGL with nanomolar potency (Labar et al., 2007), while isothiazolinone-based compounds (King et al., 2009a) and natural terpenoids (King et al., 2009b) were shown to reversibly inhibit MGL activity by targeting Cys201 and Cys208. While the localization of cysteine residues has been clarified by X-ray experiments, site-directed mutagenesis studies also shed light on the impact of residues Cys201, Cys208 and Cys242 on the enzymatic activity of human MGL (Laitinen et al., 2013). Notably, a single mutation of Cys242 to alanine was shown to impair the balance of monoglyceride isomers hydrolysis (*sn*-1 vs *sn*-2). The Cys242Ala mutation also affects the binding of the nucleophilic serine-targeting fluorophosphonate probe TAMRA-FP, used in activity-based protein profiling experiments to characterize catalytically active serine hydrolases (Cravatt et al., 2008). These findings suggest that Cys242 is necessary for substrate recognition, binding and/or enzymatic processing. On the other hand, Cys201Ala and Cys208Ala mutations do not influence the enzymatic rate and affinity of substrate for MGL (Dotsey et al., 2015). This observation is in apparent contrast to previously reported evidence highlighting the fundamental role played by Cys201 and Cys208 in the activity of specific classes of inhibitors (King et al., 2009a, King et al., 2009b; Kapanda et al., 2009), and the mechanistic role of these two cysteines deserves further investigation.

3.2. Crystal structures of human MGL

MGL belongs to the α/β hydrolase superfamily of enzymes (Karlsson et al., 1997) and several homology models have been built in an attempt to predict its structure (Saario et al., 2005; Bowman and Makriyannis, 2009; King et al., 2009a). This superfamily include ester hydrolases, peptide hydrolases, lipid hydrolases, thioester hydrolases, epoxide hydrolases, haloperoxidases, dehalogenases, and C-C bond breaking enzymes. They all share a common β -sheet core, consisting of seven parallel and one antiparallel strands, surrounded by α helices. Beside this highly conserved structure, the members of this family also present a more variable structural feature, called *lid* or *cap* domain; this domain hides the core region of the enzyme, protecting and shaping at the same time the access of substrates to the catalytic site.

Various research groups have succeeded in the crystallization of human MGL, providing an exhaustive overview of the tridimensional properties of this enzyme and the architecture of

its catalytic site. Two distinct crystal structures of the enzyme without inhibitor have been disclosed, almost simultaneously, by two independent research groups (PDB: 3JW8, Bertrand et al., 2010; PDB: 3HJU, Labar et al., 2010). Both structures present two protein molecules per asymmetric unit, each with the catalytic site facing the phospholipid membrane. In addition to the common tridimensional arrangement of α/β hydrolases – characterized by a β -sheet core surrounded by six α helices (α 1, α 2, α 3, α 6, α 7 and α 8) – MGL contains two additional helices, α 4 and α 5, which are part of the lid domain. This region comprises residues 151 to 225, that is, helix α 4, α 5, α 6 and the loops connecting α 4 to α 5 and α 5 to α 6. Within the lid domain, α 4 and the loop connecting α 4 to α 5 delineate a wide U-shaped structure that delimits the substrate access to the catalytic site.

The tridimensional structures also provide a clear description of the architecture of the enzyme active site; the catalytic triad (Ser122, Asp239 and His269) is buried below the lid domain (Figure 2). The nucleophilic Ser122 is part of the GX SXG consensus motif, situated on a turn between helix α 3 and β 5, also called “nucleophilic elbow”. As shown by the crystal structures, the catalytic residues are oriented to maximize the nucleophilic character of Ser122, forming a hydrogen-bond network that includes Asp239 and His269, His269 and Ser122. The oxyanion hole, constituted by the backbone NH groups of Ala51 and Met123, is situated on the loop connecting α 1 and β 3 and stabilizes the anionic transition state of the hydrolysis reaction. Three cysteine residues out of four have been localized, providing fundamental information about their role in the regulation of MGL activity. Cys33 is situated on β strand 2, within the α/β hydrolase core of the enzyme, far apart from the active site. On the other hand, Cys242 is in close contact with the catalytic triad, located only 4 Å away from the nucleophilic serine (Labar et al., 2010). Cys201 is situated within the loop connecting α 5 and α 6 helices. Although its side chain points toward the solvent, the lid domain is quite thin in that region and the backbone of C201 is also accessible from the active site. Cys208 is found at the top of helix α 6, with the thiol group pointing toward the cytosol (Labar et al., 2010), farther away from the active site (Figure 2). Another interesting feature highlighted by the X-ray experiments is the presence of a small opening of 5 Å connecting the active site and the solvent outside the enzyme. This hole is delimited by the lid domain, being bordered by residues Pro178, Ser181, Leu184, Tyr194, Asn195, Arg202 and Ala203 situated on the loops connecting α 4 to α 5 and α 5 to α 6 helices. Due to its close proximity to the catalytic site, this aperture may provide an exit route for the glycerol moiety released after 2-AG cleavage.

The crystal structures of MGL provided important information on the architecture of the substrate-binding site, laying the basis for rational drug design. The tridimensional structures revealed that the catalytic triad is housed at the bottom of a long channel delimited by hydrophobic residues. The side chains of residues Leu148, Ala164, Leu176, Ile179, Leu205, Val207, Ile211, Leu213, Leu214, Val217 and Leu241 shape the wall of this cavity, which is thought to accommodate the lipophilic chain of 2-AG, and helix α 4 and the loop connecting helices α 4 and α 5 delineate the U-shaped access of this cavity. Interestingly, in the crystal structure 3JW8 (Bertrand et al., 2010) this tunnel is partially filled with molecules of 2-methyl-pentane-2,4-diol (MPD), which is necessary for crystal growth; four molecules of MPD are present in monomer A, and three in monomer B. The authors suggest that the presence of MPD molecules in the tunnel supports the hypothesis that the endogenous

substrate could be extracted from the membrane, and accommodated with the polar head pointing towards the catalytic site. At the lower extremity of the hydrophobic tunnel the environment of the catalytic triad becomes more hydrophilic. Beside the oxyanion hole formed by backbone nitrogen atoms of Ala51 and Met123, the Tyr58 hydroxyl group, the imidazolic nitrogens of His121 and 272, the guanidinium group of Arg57, the carboxylate of Glu53 and the backbone of Ala 51 delineate a polar cleft. In the crystal structure 3HJU (Labar et al., 2010) this cavity accommodates a glycerol molecule, used as cryoprotectant in the purification protocol. The glycerol molecule is situated at the entrance of this cleft, with its hydroxyl groups making hydrogen bonds with the Ala51 carbonyl, Glu53 carboxylate and the hydroxyl group of Tyr94. The fact that this alcohol-binding pocket is found in close proximity of the hypothetical exit route for glycerol suggests that it might bind the polar head of 2-AG within the active site.

The crystal structures of MGL in complex with different inhibitors provided further insights into the properties of the enzyme active site. Two crystal structures of MGL covalently bound to carbamate-based inhibitors (PDB ID: 3JWE, Bertrand et al., 2010; 4UUQ, Griebel et al., 2015; Figure 3, panel A), and the crystal structure of MGL in complex with a reversible inhibitor (PDB ID: 3PE6, Schalk-Hihi et al., 2011; Figure 3, panel B) are available. 3JWE is the crystal structure of MGL in complex with SAR629 (Hornaert, 2011), which inhibits the enzyme by mimicking the pathway of 2-AG cleavage and making a stable carbamate adduct with Ser132 (Ser122 in 3HJU). Similarly to what observed in the crystal structures with no inhibitor, 3JWE presents two molecules per asymmetric unit, with the two monomers oriented in a specular way. The tridimensional structure also reveals that SAR629 adopts the same conformation in both monomers. In spite of this similarity, there is no electron density for the helix $\alpha 4$ of monomer A, while this helix shows a stable conformation in monomer B. Moreover, in monomer B a second SAR629 molecule has been found; this molecule is situated at the top of the access tunnel, and it is unlikely to play any role in inhibition. Notably, the conformation of helix $\alpha 4$ of the monomer B corresponds to that observed in the crystal structure of empty MGL 3JW8, obtained under the same conditions (Bertrand et al., 2010). The inhibitor molecules adopt a “Y shape”, spanning the lipophilic portion of the enzyme within the access tunnel; one of the fluorophenyl rings fits a hydrophobic pocket delimited by Leu158, Leu223 and Leu224 (respectively Leu148, Leu213 and Leu214 in 3HJU), while the second fluorophenyl moiety is in contact with Leu186, Leu189 and Leu215 (Leu176, Leu179 and Leu205 in 3HJU). The interaction between MGL and SAR629 is thus mainly mediated by hydrophobic contacts, while there is only one direct polar interaction between the carbonyl oxygen of SAR629 and the nitrogen atoms of the oxyanion hole (Ala61 and Met133, Ala51 and Met123 in 3HJU).

A crystal structure of MGL in complex with the covalent inhibitor SAR127303 has been resolved very recently (PDB: 4UUQ, Griebel et al., 2015). As in the case of the complex MGL-SAR629 (3JWE), the complex MGL-SAR127303 is crystallized with two protein molecules per asymmetric unit, showing a specular orientation of the two monomers. Contrary to SAR629, SAR127303 does not have a Y-shaped structure. The binding mode of the inhibitor within the MGL lipophilic tunnel is slightly different in the two monomers, which in turn show structural differences in their lid domains. More specifically, while the structural arrangement of monomer B corresponds to that observed in the empty (3HJU),

3JW8) and in the inhibited MGL (3JWE) crystal structures previously reported, monomer A of 4UUQ shows structural variances concerning the loop connecting the $\beta 6$ strand to helix $\alpha 4$. These rearrangements determine a small reduction of the U-shaped opening of the lid domain in monomer B, which thus makes different interactions with the inhibitor. The sulfonyl group of SAR127303 adopts different orientations; in both monomers this group makes a polar interaction between an oxygen atom and the Asn162 (Asn152 in 3HJU) backbone nitrogen. In monomer A, but not in monomer B, this oxygen atom also makes water-mediated interactions with Asn162 side chain and Leu251 (Leu241 in 3HJU) backbone oxygen. The chlorophenyl group accommodates in a hydrophobic pocket delimited by residues Leu215, Gly220, Leu223, Leu224 Ala166 and Ser165. The existence of two alternative binding modes might be due to the flexibility of the lid domain, and specifically of the loop connecting the $\beta 6$ strand and $\alpha 4$, to which Asn162 belongs.

A further crystal structure of MGL in complex with a non-covalent reversible inhibitor has been solved in 2011 (PDB: 3PE6; Schalk-Hihi et al., 2011). The authors mutated MGL at different sites, to obtain a more soluble form of the enzyme and identify optimal conditions for crystallization in absence of detergents. The best result is the human MGL Lys36Ala, Leu169Ser and Leu176Ser; these residues are situated on the $\beta 1$ strand, on helix $\alpha 4$ and on the loop connecting helix $\alpha 4$ to $\alpha 5$, respectively. The crystal structure of 3PE6 reveals that the binding site is almost entirely occupied by the non-covalent inhibitor ZYH. The amide carbonyl of ZYH is oriented to make polar contacts with Met123 within the oxyanion hole environment. The 3-(4-(pyrimidin-2-yl)piperazin-1-yl)azetidiny moiety is situated in the alcohol-binding pocket described above, which is filled with a glycerol molecule in 3HJU. The 2-cyclohexylbenzoxazol-6-yl portion extends in the lipophilic tunnel, occupying approximately the same region that accommodates the covalent inhibitors SAR127303 and SAR629, making van der Waals-mediated interactions with the protein. Notably, this crystal structure reveals a substantial conformational rearrangement involving the helix $\alpha 4$ of the lid domain. The authors described the new architecture of the lid domain as a closed conformation, compared to the open conformation observed in 3HJU. The transition from the empty/open form to the ligand-bound/closed form consists in a rolling motion of the helix $\alpha 4$ over the catalytic site; moreover, the conformational change also involves the incorporation in helix $\alpha 4$ of residues 153–157, which belong to the loop connecting strand $\beta 6$ and helix $\alpha 4$ in all the other crystal structures. At the opposite tip of helix $\alpha 4$, the loop region that comprises residues 174–182 assumes a substantially different conformation, moving upward from the conformation adopted in the other crystallized structures. The overall effect of these rearrangements is an approaching movement of the lid domain rims, leading to a narrowed access to the catalytic site; moreover, the glycerol exit hole, described as an open cavity in 3HJU, 3JW8 and 3JWE, is completely closed.

The available crystal structures provide important clues about the function of the lid domain. As already mentioned, this domain is composed by residues 151–225 (Schalk-Hihi et al., 2011); other authors (Bertrand et al., 2010) refer to the lid domain as a more restricted region, consisting of the helix $\alpha 4$ and the loop connecting helices $\alpha 4$ and $\alpha 5$. As revealed by the available crystal structures, helix $\alpha 4$ consists of residues 157–170, with the only exception of crystal 3PE6, in which this helix is more extended, and includes residues 153–157, as a consequence of ligand-dependent conformational changes (Figure 2). Helix $\alpha 4$ is

mainly composed of hydrophobic residues, which orient their side chains outside the access tunnel; these residues and those situated on the loop connecting helices $\alpha 4$ and $\alpha 5$ (Leu174, Leu176 and Leu179) delimit a hydrophobic region at the surface of MGL. Notably, the lid domain of MGL is characterized by a more marked hydrophobic character compared to that of other members of the α/β hydrolases superfamily. On the other hand, MGL has been found both in the cytosol and membrane fraction of Cos-7 cells (Dinh et al., 2002). Together, these findings lead to the conclusion that MGL acts in cells as an amphitropic protein, soluble in the cytosol and, at the same time, able to interact with the phospholipid membrane to recruit its lipophilic substrate (Labar et al., 2010). The presence of three additional hydrophilic residues situated on helix $\alpha 4$ – Asn152, Glu154 and Lys160 – might mediate the interaction of the enzyme with the polar head of 2-AG; moreover, the positively charged Lys160 could also interact with the phosphate groups of membrane phospholipids.

The comparison with the tridimensional structures of other lipases, such as dog gastric lipase and human pancreatic lipase, revealed substantial structural diversities due to different functions, and helped shed light on the relationship between the architecture of MGL's lid domain and its biological function (Labar et al., 2010). In many lipases, including MGL, the lid domain covers the active site, partially reducing its exposure to the solvent. Moreover, it has been hypothesized that the lid domain of human pancreatic lipase undergoes conformational variations in the presence of a water-lipid interface, disclosing the access to the hydrophobic binding site when the protein interacts with lipid droplets. This phenomenon, often referred to as “interfacial activation”, has been extensively studied for lipases (Cambillau et al., 1996; Aloulou et al., 2006; Reis et al., 2009), and allows the enzyme to exist in two distinct conformations – closed and open – which correspond to inaccessible or solvent-exposed active site. The lid domain structure appears thus to be strictly related to the enzyme functions. These evidences, and the existence of different MGL crystal structures showing different lid domain conformations (Figure 2), suggest that MGL might regulate the access of 2-AG to the catalytic site through a flexible control on the lid domain opening.

The crystal structures 3HJU and 3JW8 show MGL in its open conformation; however, while the open conformation of 3HJU could have been stabilized by detergents used in the purification protocol (Labar et al., 2010), the presence of crystal soaking adjuvant molecules might have played a role in stabilizing the helix $\alpha 4$ in 3JW8 (Bertrand et al., 2010). Moreover, the helix $\alpha 4$ of monomer B in 3HJU is poorly defined, as a further proof of the lid domain flexibility and, in the first crystal structure of MGL covalently bound to an inhibitor, 3JWE (Bertrand et al., 2010), the helix $\alpha 4$ of monomer A had not been solved. Two other crystal structures of MGL in complex with different inhibitors clearly show that the helix $\alpha 4$ of the lid domain can exist in different conformations. The access to the catalytic site of monomer B in 4UUQ is partially occluded, due to a rearrangement of the flexible loop connecting β strand 6 to helix $\alpha 4$ (Griebel et al., 2015). Moreover, 3PE6 shows a remarkable change in the lid domain structure, due to the movement of helix $\alpha 4$ over the active site access, leading to a partially closed conformation (Schalk-Hihi et al., 2011). Interestingly, Schalk-Hihi and coworkers also showed that, beside the structural rearrangement, the transition from the open to the closed conformation implies a reduction of the hydrophobic character of the lid domain. While a full understanding of the functional

significance of helix $\alpha 4$ requires additional investigation, the authors hypothesized that the hydrophobic character of this region might serve to position the enzyme in close contact with the phospholipid membrane, in order to facilitate the recruitment of 2-AG. According to this model, following substrate binding helix $\alpha 4$ closes the active site access, and MGL dissociates from the membrane while cleaving 2-AG. Finally, after substrate cleavage the enzyme might assume again the open conformation and re-associate to the membrane. Thus, the catalytic cycle would happen concomitantly to reversible conformational rearrangements of the lid domain.

4. MGL inhibitors

4.1 Relevance of MGL inhibitors

2-AG participates in a wide range of physiological and pathological processes. The role of 2-AG in neural systems that alleviate pain has been extensively studied and it has been convincingly shown that 2-AG promotes antinociception by acting both in the CNS (Hohmann et al., 2005; Connell et al., 2006) and the periphery (Guindon et al. 2011; Guindon et al., 2013). 2-AG-mediated activation of cannabinoid receptors is also responsible for neuroprotection and prevention of neural inflammation following tissue damage (Kreutz et al., 2009; Carloni et al., 2012; Xu and Chen, 2015) and in neuronal disease models (Chen et al., 2012; Piro et al., 2012; Zhang et al., 2014; Fernández-Suárez et al., 2014; Lysenko et al., 2014). Endocannabinoid signaling, including 2-AG-mediated signaling, plays a key role in the control of anxiety and depression and the regulation of emotional memory (Sciolino et al., 2011; Shonesy et al., 2014). Finally, endocannabinoids may have a role as anticancer compounds: overexpression of CB_1 receptors has been observed in several tumors, providing evidence that 2-AG might be implicated in cancer growth and aggressiveness. Moreover, MGL is abnormally expressed in various human cancer cells and primary high-grade tumors. Pharmacological and genetic ablation of MGL has been found to reduce migration, invasiveness of cancer cells and tumor growth *in vivo* (Nomura et al., 2010; Nomura et al., 2011). Interestingly, the role of MGL in promoting cancer pathogenesis is related not only to its role in 2-AG levels regulation, but also to its ability to interfere with multiple cellular mechanism and metabolic routes. Indeed, MGL activity controls the levels of fatty acids as precursors of lysophosphatidic acid and eicosanoids, which in turn activate tumor-promoting paths. MGL blockade is thus sufficient to reduce the production of lipid modulators involved in cancer pathogenicity (Nomura et al., 2010; Nomura et al., 2011). While in ovarian, breast and melanoma cancer cells MGL inhibition exerts an anti-tumorigenic effect through the reduction of oncogenic signaling lipids, in prostate cancer cells MGL blockade-dependent anti-cancer effects are mediated by both enhanced CB_1 signaling and impaired lipid network. Moreover, MGL inhibition is responsible for the downregulation of cyclin D1 and Bcl-2, involved in colorectal cancer pathogenesis (Ye et al., 2011).

The regulation of 2-AG levels thus represents a challenging goal from a medicinal chemistry point of view, and in the last decade, a special effort has been made to discover selective and potent MGL inhibitors. However, while several beneficial effects have been observed for MGL blockade both *in vitro* and *in vivo*, doubts about the use of MGL inhibitors arose, due

to the adverse effects observed. MGL chronic inhibition causes functional antagonism of CB₁ receptors in the brain (Schlosburg et al., 2010), which can in turn lead to neuropsychiatric effects such as anxiety and depression. Recent studies have shown that irreversible MGL inhibitors produce a deterioration of learning performances and loss of memory function, related to a decrease of long-term potentiation of CA1 synaptic transmission and acetylcholine levels (Griebel et al., 2015).

4.2 URB602 and derivatives

The *O*-biphenylcarbamate URB602 (IC₅₀ = 223 μM; Figure 4) was the first MGL-preferring inhibitor to be reported (Hohmann et al., 2005). In spite of its low potency, URB602 elevates *in vivo* the levels of 2-AG, but not anandamide, and enhances CB₁ receptor-mediated stress-induced analgesia (Hohmann et al., 2005). Moreover, URB602 exerts peripherally mediated antinociceptive effects in various models of pain (Hohmann et al., 2005; Costa et al., 2007; Desroches et al., 2008). Kinetic analyses revealed that URB602 inhibits rat MGL through a non-competitive mechanism; further work demonstrated that the inhibition is time-independent and that URB602 does not mimic the substrate (King et al., 2007). Dialysis after incubation of purified MGL in presence of the inhibitor partially reversed the inhibition of enzymatic activity, pointing to a partially reversible mechanism of action (King et al., 2007). Notably, King and coworkers also found that a ureidic derivative of URB602 is more potent than the parent compound (IC₅₀ = 115 μM). While this compound is characterized by high steric similarity with URB602, the ureidic group shows a lower tendency to react with the catalytic serine (Ser122), suggesting that these compounds are not site-directed inhibitors.

In an attempt to enhance the potency of *O*-biphenylcarbamate compounds, Szabo and coworkers synthesized and tested as potential MGL inhibitors a broad series of URB602 derivatives (Szabo et al., 2008). The authors extensively explored different modifications of URB602, including isosteric replacements, ring size and substitution, *para*-substitution of the biphenyl moiety and the incorporation of a bicyclic element, and found a *p*-OH substituted derivative showing higher potency at inhibiting MGL. Molecular modeling suggested that the *p*-OH derivative could accommodate in the upper part of the access tunnel, while the hydroxyl group takes polar interaction with Ser185. Furthermore, the ureidic analogue of the new compound maintained moderate MGL inhibition activity, supporting the carbamate and the urea functionalities as promising scaffolds for the development of MGL inhibitors.

4.3 JZL184 and other inhibitors that target the catalytic site

The application of competitive activity-based protein profiling (ABPP) led to the discovery of the piperidine-carbamate compound JZL184 (Long et al., 2009a; Figure 4). JZL184 inhibits MGL activity with an IC₅₀ of 8 nM, and blocks MGL *in vivo* causing a considerable increase of 2-AG levels in the brain. As shown by liquid chromatography tandem-mass spectrometry, JZL184 inhibits MGL through the formation of a covalent adduct with the nucleophilic Ser122 (Long et al., 2009b); this complex is stable against hydrolysis, and is responsible for irreversible inhibition of the enzyme. Notably, JZL184 shows a relatively high selectivity for MGL over FAAH (about 100 fold) and other hydrolases present in

mouse brain (Long et al., 2009b). On the other hand, the compound shows inhibitory activity towards other carboxylesterases in peripheral tissues, cross-reactivity for FAAH after repeated administration, and is characterized by low cross-species activity, showing lower potency for rat MGL than mouse MGL (Long et al., 2009b). Although acute blockade of MGL by JZL184 exerts a broad range of potentially beneficial effects, repeated administration of the compound results in desensitization of CB₁ receptors, cross-tolerance to CB₁ receptor agonists along with tolerance to the antinociceptive effects exerted by the compound, physical dependence, and impaired endocannabinoid-dependent synaptic plasticity (Schlosburg et al., 2010). Although more recent work suggests that these effects may be tempered by a low-dose administration protocol (Kinsey et al., 2013), these liabilities hamper the clinical development of JZL184 and limit its use as an experimental probe of MGL activity. The class of 4-nitrophenyl carbamates is rather promiscuous, as shown by the FAAH/MGL dual inhibitor, JZL195 (Long et al., 2009c).

To develop MGL inhibitors with improved selectivity and cross-species activity, new compounds with *O*-hexafluoroisopropyl carbamate (Chang et al., 2012; Chang et al., 2013) or *N*-hydroxysuccinimidyl carbamate functionalities have been studied (Niphakis et al., 2013). KML29 is an *O*-hexafluoroisopropyl analog of JZL184 (Chang et al., 2012); interestingly, the substitution of the *p*-nitrophenyl leaving group with a hexafluoroisopropyl one was apparently sufficient to achieve complete selectivity for MGL over FAAH and other brain hydrolases, while maintaining a remarkable inhibitory activity towards mouse MGL (IC₅₀=15 nM). KML29 and JZL184 showed similar dose-dependent MGL inhibition *in vivo*, giving maximal inhibition at 20 mg/Kg dose; JZL184 was found to inhibit FAAH at higher doses (40 mg/Kg), while KML29 maintained complete selectivity over FAAH at all doses (Chang et al., 2012). Moreover, contrary to what had been observed for JZL184, KML29 inhibits both rat and human MGL, showing an improved cross-species activity. Yet more recent work disclosed JW651, a close analog of KML29, as a selective MGL inhibitor with *in vitro* and *in vivo* activities (Chang et al., 2013). The fact that JZL184 and KML29 show differences limited to the leaving group suggests that the introduction of a bioisosteric moiety, able to mimic the polar head of the endogenous substrate, and modulation of its reactivity might represent a promising strategy for the development of potent and selective site-directed MGL inhibitors. However, KML29 induced mild cannabimimetic effects when administered *in vivo* to mice (Pasquarelli et al. 2015).

Recently, Griebel and coworkers reported a detailed characterization of SAR127303 (Figure 2, panel A), a potent *O*-hexafluoroisopropyl carbamate (Griebel et al., 2015). While sharing the same leaving group and piperidine carbamate functionalities as KML29, this compound is characterized by a different substituent at the piperidine ring, which occupies the rear part of the access tunnel, as revealed by the crystal structure of the covalent complex with MGL (PDB: 4UUQ). SAR127303 is a potent inhibitor of mouse and human MGL (IC₅₀=3.8 nM and 29 nM respectively) and shows high selectivity for MGL over other human hydrolases. SAR127303 exerts antinociceptive effects in inflammatory and visceral pain models as well as antiepileptic effects. Despite the typical beneficial effects related to MGL inhibition, however, SAR127303 negatively affects memory formation, leading to impaired cognitive

performance and deficiencies in acquisition and consolidation processes in spatial, episodic and working memory.

Selective inhibitors of MGL composed by a piperidine or piperazine ring with a putative serine-carbamoylating functionality include triazoleureas, such as JJKK-048 (Aaltonen et al., 2013, Figure 4), and *N*-Hydroxysuccinimidyl carbamates, such as MJN110 (Niphakis et al., 2013, Figure 4). Other compounds with serine-reactive groups, such as tetrazolylureas (Ortar et al. 2013) and 1,3,4-oxadizol-3-ones (Käsnänen et al. 2013) had shown MGL-inhibitor activity, but these classes generally showed also inhibition of other serine hydrolases like FAAH. Recently, a compound lacking reactive functionalities, CL6a (Tuccinardi et al. 2014, Figure 4) has been described as a micromolar reversible inhibitor of MGL, addressing the catalytic pocket, similarly to what had been observed for the crystal structure with the non-covalent inhibitor ZYH (Figure 2), and a lipophilic ester (Hernandez-Torres et al., 2014, Comp21 in Figure 4) has been shown to inhibit MGL with sub-micromolar potency.

4.4 Cysteine-targeting compounds

4.4.1 *N*-substituted maleimide derivatives—Starting from experimental evidence indicating that MGL contains one or more sulfhydryl sensitive sites, Saario and coworkers synthesized and tested a broad series of *N*-ethylmaleimide derivatives as potential MGL inhibitors (Saario et al., 2005), with the aim of characterizing the mechanism of action and the role of the *N*-substituent. Interestingly, derivatives with bulkier and more lipophilic substituents, such as propyl, cyclohexyl, phenyl and pyrenyl groups, show enhanced selectivity, suggesting that the sulfhydryl sensitive site in MGL may be situated in a hydrophobic environment. On the other hand, the authors found that *N*-arachidonylemaleimide (NAM, Figure 5), a derivative that is structurally similar to the endogenous substrate 2-AG, was the most potent compound in the series (IC₅₀=140 nM). More recently, Matuszak and coworkers confirmed this finding through a further investigation of various alkyl-phenyl *N*-substituents (Matuszak et al., 2009).

Because they are Michael acceptors, NAM and other *N*-substituted maleimide derivatives are irreversible MGL inhibitors. Mass spectrometry and mutagenesis experiments revealed that inhibition of human MGL by NAM is mediated by the Michael addition of the arachidonylemaleimide group to Cys201 and Cys242 (Zvonok et al., 2008a/b; King et al., 2009a; Laitinen et al., 2013).

4.4.2 Disulfide compounds—To further characterize the role of cysteine residues in the modulation of MGL activity, Labar and coworkers tested the activity of various disulfide compounds, including disulfiram, disulfiram analogues and phenyl disulfide (Labar et al. 2007). The compounds inhibit human MGL in a concentration-dependent manner with IC₅₀ values of 6.44±0.05 μM (disulfiram), 6.87±0.05 μM (dicyclopentamethylthiuram disulfide, Figure 5) and 5.79±0.05 μM (phenyl disulfide). The authors hypothesized that disulfide compounds might react with cysteine residues in MGL through a redox process that required the formation of a mixed disulfide. Consistent with this idea, bis(dialkylaminethiocarbonyl)disulfide derivatives were shown to inhibit hMGL activity

through a redox mechanism involving the sulfhydryl groups of Cys208 and, to a lesser extent, Cys242 (Kapanda et al., 2009). Results showing that disulfide-dependent MGL inactivation is completely restored by dithiothreitol (DTT) corroborate the hypothesis that the chemical control of the redox state of critical cysteine residues represents a feasible alternative to site-directed MGL inhibition.

4.4.3 Isothiazolinone and benzisothiazolinone derivatives—The observation that sulfhydryl reagents are potent MGL inhibitors also led to the discovery of isothiazolinone and benzisothiazolinone derivatives as potent and selective modulators of MGL activity (King et al., 2009a). A series of different cysteine-reacting compounds were screened to test their potential as MGL inhibitors, and 2-octyl-4-isothiazolin-3-one (octhilinone, Figure 5) was found to be potent in that respect ($IC_{50}=88\pm 12$ nM on rat MGL). Substitution of the *N*-octyl group with a methyl group caused a reduction in inhibitory potency, while the introduction of more lipophilic and larger substituents, such as an oleoyl group, enhanced it ($IC_{50}=43\pm 8$ nM). Replacement of the isothiazolinone functionality with a benzisothiazolinone group (Figure 5) also led to a potent inhibitor, suggesting that inhibition of MGL mediated by these compounds does not rely on the formation of Michael adducts. Rapid dilution assays showed indeed that octhilinone inhibits MGL activity through a partially reversible mechanism. These lines of evidence and the fact that low concentrations of DTT are able to reduce the potency of octhilinone, while not directly affecting enzyme activity, led to the conclusion that isothiazolinone and benzisothiazolinone derivatives might inhibit MGL through the formation of a disulfide bond between the sulphenamide group and a cysteine residue of the protein. Furthermore, mutation of Cys242 to glycine, but not Cys201Gly or Cys208Gly mutations, resulted in a marked decrease in the inhibitory activity of octhilinone, which is suggestive of a preferential interaction of this inhibitor with Cys208. The mechanism of isothiazolinone and benzisothiazolinone-mediated human MGL inhibition has been investigated (Matuszak et al., 2011). Octhilinone and *N*-octylbenzisothiazolinone were shown to have lower potency toward hMGL than rMGL, while conserving high selectivity for MGL over FAAH. Increasing DTT additions completely restored the enzyme activity, confirming the cysteine-based mechanism proposed by King and colleagues. On the other hand, the authors provided mutagenesis data showing that, contrary to what observed for octhilinone, both Cys242Ala and Cys201Ala mutations determine a decrease in the potency of *N*-octylbenzisothiazolinone, while Cys208Ala mutation does not affect the inhibitor potency. Notably, for both octhilinone and *N*-octylbenzisothiazolinone, the simultaneous mutation of Cys201, Cys208 and Cys242 determines a remarkable reduction of their potency on human MGL. Together, these results have improved our knowledge about regulatory cysteine residues, which are not directly involved in the enzymatic activity of MGL, and revealed benzisothiazolinone-based compounds as potential MGL inhibitors.

4.4.4 Natural terpenoids as MGL inhibitors—Searching for new scaffolds that might be used to design reversible MGL inhibitors, King and coworkers found two naturally occurring terpenoids, pristimerin and euphol, which showed high potency and selectivity (King et al., 2009b). Pristimerin ($IC_{50}=93\pm 8$ nM; Figure 5) is a pentacyclic triterpenoid characterized by a quinone-methide group, which could react with cysteine residues yielding

covalent adducts. However, as revealed by rapid dilution assays, pristimerin-dependent inhibition of rat MGL is completely reversible. Kinetic data showed that pristimerin reduces the maximum catalytic activity of the enzyme, but does not affect its Michaelis-Menten constant, which defines it as a rapid reversible and non-competitive inhibitor. In an attempt to characterize the role of the quinone-methide functionality, the authors tested as a potential MGL inhibitor euphol, a terpenoid that lacks the quinone-methide group of pristimerin, while having a very similar 3D shape. Although euphol is less potent than pristimerin ($IC_{50} = 315 \pm 1$ nM), kinetic experiments and rapid dilution assays showed that it also inhibits MGL through a non-competitive and reversible mechanism. Interestingly, mutation of Cys201 or Cys208 affected the inhibitory potency of these compounds, although in different manners: Cys208Gly mutation reduced the potency of pristimerin without affecting that of euphol; conversely, Cys201Gly mutation decreased the inhibitory potency of euphol, but not that of pristimerin. Docking simulations with a homology-based model of MGL structure suggested that both euphol and pristimerin could occupy a hydrophobic pocket within the lid domain, but these simulations should be re-evaluated in light of the crystal structures that have been published after that work. Incubating primary cultures of rat cortical neurons with the terpenoid caused an increase in 2-AG levels, without any effect on levels of the FAAH substrate palmitoylethanolamide. On the other hand, although it does not affect FAAH or NAAA (*N*-acylethanolamine acid amidase) activities, pristimerin was found to be a potent inhibitor of ABHD-6 ($IC_{50} = 98 \pm 8$ nM).

More recently, a pentacyclic terpenoid structurally similar to pristimerin, β -amyryn, was shown to inhibit human MGL with an IC_{50} of 2.8 μ M (Chicca et al., 2012) confirming that natural triterpendoids scaffolds may offer novel ways for the discovery of MGL inhibitors. Rapid dilution assay and kinetics experiments revealed that, as previously observed for pristimerin (King et al., 2009b), β -amyryn inhibits MGL through a rapid, reversible and non-competitive mechanism. Notably, β -amyryn treatment determines an increase of intracellular 2-AG levels, but does not affect the levels of other endocannabinoids, suggesting that this compound selectively targets 2-AG hydrolysis. On the other hand, further measurements of amyryn-dependent increase in 2-AG levels showed that β -amyryn exerts a combined inactivation of the enzymes degrading 2-AG, inhibiting MGL, ABHD6 and ABHD12.

5. Conclusions

The fundamental role played by MGL in the degradation of the endocannabinoid 2-AG identifies this enzyme as a potential target for pharmacological agents able to treat such diverse pathological conditions as cancer, chronic pain and Alzheimer's disease. In the last decade, a great deal of effort has been put in the development of potent and selective MGL inhibitors, arriving to the discovery of compounds that have become important pharmacological tools for the identification and characterization of the biological effects caused by MGL blockade. While the beneficial effects associated with MGL inhibition have begun to emerge, serious potential liabilities have also been discovered. There is clear evidence that chronic inhibition of MGL causes a functional antagonism of brain CB_1 receptors and produces a variety of undesired effect, including physical dependence. Thus, the need to discover selective and reversible MGL inhibitors remains urgent. The identification of critical cysteine residues that are able to regulate MGL activity, although

not directly involved in the enzymatic process, is of interest in this context as it might lead to develop allosteric modulators endowed with greater selectivity and fewer side effects. In this perspective, the characterization of MGL 3D-structures facilitated the rational design of novel MGL inhibitors. In spite of this, while an exhaustive description of the active site architecture has been provided, the structural basis for the conformational plasticity of the lid domain is still largely unknown. One possibility is that this structure serves as a flexible gate into the active site during the catalytic cycle of the enzyme. However, the events that trigger its opening and closing remain mysterious.

References

- Aaltonen N, Savinainen JR, Ribas CR, Rönkkö J, Kuusisto A, Korhonen J, Navia-Paldanius D, Häyrynen J, Takabe P, Käsnänen H, Pantsar T, Laitinen T, Lehtonen M, Pasonen-Seppänen S, Poso A, Nevalainen T, Laitinen JT. Piperazine and piperidine triazole ureas as ultrapotent and highly selective inhibitors of monoacylglycerol lipase. *Chem Biol.* 2013; 20:79–90.
- Aguado Y, Monory K, Palazuelos J, Stella N, Cravatt B, Lutz B, Marsicano G, Kokaia Z, Guzmán M, Galve-Roperh I. The endocannabinoid system drives neural progenitor proliferation. *FASEB J.* 2005; 19:1704–1706. [PubMed: 16037095]
- Aguado T, Palazuelos J, Monory K, Stella N, Cravatt B, Lutz B, Marsicano G, Kokaia Z, Guzmán M, Galve-Roperh I. The endocannabinoid system promotes astroglial differentiation by acting on neural progenitor cells. *J Neurosci.* 2006; 26:1551–1561. [PubMed: 16452678]
- Aloulou A, Rodriguez JA, Fernandez S, van Oosterhout D, Puccinelli D, Carrière F. Exploring the specific features of interfacial enzymology based on lipase studies. *Biochim Biophys Acta.* 2006; 1761:995–1013. [PubMed: 16931141]
- Beltramo M, Piomelli D. Carrier-mediated and enzymatic hydrolysis of the endogenous cannabinoid 2-arachidonoylglycerol. *Neuroreport.* 2000; 11:1231–1235. [PubMed: 10817598]
- Bertrand T, Augé F, Houtmann J, Rak A, Vallée F, Mikol V, Berne PF, Michot N, Cheuret D, Hoornaert C, Mathieu M. Structural basis for human monoglyceride lipase inhibition. *J Mol Biol.* 2010; 396:663–673. [PubMed: 19962385]
- Bisogno T, Howell F, Williams G, Minassi A, Cascio MG, Ligresti A, Matias I, Schiano-Moriello A, Paul P, Williams E-J, Gangadharan U, Hobbs C, Di Marzo V, Doherty P. Cloning of the first sn1-DAG lipases points to the spatial and temporal regulation of endocannabinoid signaling in the brain. *J Cell Biol.* 2003; 163:463–468. [PubMed: 14610053]
- Blankman JL, Simon GM, Cravatt BF. A comprehensive profile of brain enzymes that hydrolyze the endocannabinoid 2-arachidonoylglycerol. *Chem Biol.* 2007; 14:1347–1356. [PubMed: 18096503]
- Blankman JL, Long JZ, Trauger SA, Siuzdak G, Cravatt BF. ABHD12 controls brain lysophosphatidylserine pathways that are deregulated in a murine model of the neurodegenerative disease PHARC. *Proc Natl Acad Sci USA.* 2013; 110:1500–1505. [PubMed: 23297193]
- Bortolato M, Mangieri RA, Fu J, Kim JH, Arguello O, Duranti A, Tontini A, Mor M, Tarzia G, Piomelli D. Antidepressant-like activity of the fatty acid amide hydrolase inhibitor URB597 in a rat model of chronic mild stress. *Biol Psychiatry.* 2007; 62:1103–1110. [PubMed: 17511970]
- Bowman AL, Makriyannis A. Refined homology model of monoacylglycerol lipase: toward a selective inhibitor. *J Comput Aided Mol Des.* 2009; 23:799–806. [PubMed: 19543978]
- Cambillau C, Longhi S, Nicolas A, Martinez C. Acyl glycerol hydrolases: inhibitor, interface and catalysis. *Curr Opin Struct Biol.* 1996; 6:449–455. [PubMed: 8794161]
- Carlioni S, Alonso-Alconada D, Girelli S, Duranti A, Tontini A, Piomelli D, Hilario E, Alvarez A, Balduini W. Pretreatment with the monoacylglycerol lipase inhibitor URB602 protects from the long-term consequences of neonatal hypoxic-ischemic brain injury in rats. *Pediatr Res.* 2012; 72:400–406. [PubMed: 22821058]
- Chang JW, Niphakis MJ, Lum KM, Cognetta AB 3rd, Wang C, Matthews ML, Niessen S, Buczynski MW, Parsons LH, Cravatt BF. Highly selective inhibitors of monoacylglycerol lipase bearing a

- reactive group that is bioisosteric with endocannabinoid substrates. *Chem Biol.* 2012; 19:579–588. [PubMed: 22542104]
- Chang JW, Cognetta AB 3rd, Niphakis MJ, Cravatt BF. Proteome-wide reactivity profiling identifies diverse carbamate chemotypes tuned for serine hydrolase inhibition. *ACS Chem Biol.* 2013; 8:1590–1599. [PubMed: 23701408]
- Chen R, Zhang J, Wu Y, Wang D, Feng G, Tang YP, Teng Z, Chen C. Monoacylglycerol lipase is a therapeutic target for Alzheimer's disease. *Cell Rep.* 2012; 2:1329–1339. [PubMed: 23122958]
- Chicca A, Marazzi J, Gertsch J. The antinociceptive triterpene β -amyryn inhibits 2-arachidonoylglycerol (2-AG) hydrolysis without directly targeting cannabinoid receptors. *Br J Pharmacol.* 2012; 167:1596–1608. [PubMed: 22646533]
- Clapper JR, Moreno-Sanz G, Russo R, Guijarro A, Vacondio F, Duranti A, Tontini A, Sanchini S, Sciolino NR, Spradley JM, Hohmann AG, Calignano A, Mor M, Tarzia G, Piomelli D. Anandamide suppresses pain initiation through a peripheral endocannabinoid mechanism. *Nat Neurosci.* 2007; 13:1265–1270. [PubMed: 20852626]
- Comelli F, Giagnoni G, Bettoni I, Colleoni M, Costa B. The inhibition of monoacylglycerol lipase by URB602 showed an anti-inflammatory and anti-nociceptive effect in a murine model of acute inflammation. *Br J Pharmacol.* 2007; 152:787–794. [PubMed: 17700715]
- Connell K, Bolton N, Olsen D, Piomelli D, Hohmann AG. Role of the basolateral nucleus of the amygdala in endocannabinoid-mediated stress-induced analgesia. *Neurosci Lett.* 2006; 397:180–184. [PubMed: 16378681]
- Cravatt BF, Wright AT, Kozarich JW. Activity-based protein profiling: from enzyme chemistry to proteomic chemistry. *Annu Rev Biochem.* 2008; 77:383–414. [PubMed: 18366325]
- Crowe MS, Leishman E, Banks ML, Gujjar R, Mahadevan A, Bradshaw HB, Kinsey SG. Combined inhibition of monoacylglycerol lipase and cyclooxygenases synergistically reduces neuropathic pain in mice. *Br J Pharmacol.* 2015; 172:1700–1712. [PubMed: 25393148]
- Desroches J, Guindon J, Lambert C, Beaulieu P. Modulation of the anti-nociceptive effects of 2-arachidonoyl glycerol by peripherally administered FAAH and MGL inhibitors in a neuropathic pain model. *Br J Pharmacol.* 2008; 155:913–924. [PubMed: 18695638]
- Devane WA, Hanus L, Breuer A, Pertwee RG, Stevenson LA, Griffin G, Gibson D, Mandelbaum A, Etinger A, Mechoulam R. Isolation and structure of a brain constituent that binds to the cannabinoid receptor. *Science.* 1992; 258:1946–1949. [PubMed: 1470919]
- Di Marzo V, Fontana A, Cadas H, Schinelli S, Cimino G, Schwartz JC, Piomelli D. Formation and inactivation of endogenous cannabinoid anandamide in central neurons. *Nature.* 1994; 372:686–691. [PubMed: 7990962]
- Dinh TP, Carpenter D, Leslie FM, Freund TF, Katona I, Sensi SL, Kathuria S, Piomelli D. Brain monoglyceride lipase participating in endocannabinoid inactivation. *Proc Natl Acad Sci USA.* 2002a; 99:10819–10824. [PubMed: 12136125]
- Dinh TP, Freund TF, Piomelli D. A role for monoglyceride lipase in 2-arachidonoylglycerol inactivation. *Chem Phys Lipids.* 2002b; 121:149–158. [PubMed: 12505697]
- Dinh TP, Kathuria S, Piomelli D. RNA interference suggests a primary role for monoacylglycerol lipase in the degradation of 2-arachidonoylglycerol. *Mol Pharmacol.* 2004; 66:1260–1264. [PubMed: 15272052]
- Dotsey EY, Jung K-M, Basit A, Wei D, Vacondio F, Armirotti A, Mor M, Piomelli D. Peroxide-dependent MGL sulfenylation regulates 2-AG-mediated endocannabinoid signaling in brain neurons. *Chem Biol.* 2015 in press.
- Fernández-Suárez D, Celorrio M, Riezu-Boj JI, Ugarte A, Pacheco R, González H, Oyarzabal J, Hillard CJ, Franco R, Aymerich MS. The monoacylglycerol lipase inhibitor JZL184 is neuroprotective and alters glial cell phenotype in the chronic MPTP mouse model. *Neurobiol Aging.* 2014; 35:2603–2616. [PubMed: 24973119]
- Galve-Roperh I, Chirchiù V, Díaz-Alonso J, Bari M, Guzmán M, Maccarrone M. Cannabinoid receptor signaling in progenitor/stem cell proliferation and differentiation. *Prog Lipid Res.* 2013; 52:633–650. [PubMed: 24076098]
- Griebel G, Pichat P, Beesské S, Leroy T, Redon N, Jacquet A, Françon D, Bert L, Even L, Lopez-Grancha M, Tolstyk T, Sun F, Yu Q, Brittain S, Arlt H, He T, Zhang B, Wiederschain D,

- Bertrand T, Houtman J, Rak A, Vallée F, Michot N, Augé F, Menet V, Bergis OE, George P, Avenet P, Mikol V, Didier M, Escoubet J. Selective blockade of the hydrolysis of the endocannabinoid 2-arachidonoylglycerol impairs learning and memory performance while producing antinociceptive activity in rodents. *Sci Rep.* 2015; 5:7642. [PubMed: 25560837]
- Guindon J, Guijarro A, Piomelli D, Hohmann AG. Peripheral antinociceptive effects of inhibitors of monoacylglycerol lipase in a rat model of inflammatory pain. *Br J Pharmacol.* 2011; 163:1464–1478. [PubMed: 21198549]
- Guindon J, Lai Y, Takacs SM, Bradshaw HB, Hohmann AG. Alterations in endocannabinoid tone following chemotherapy-induced peripheral neuropathy: Effects of endocannabinoid deactivation inhibitors targeting fatty-acid amide hydrolase and monoacylglycerol lipase in comparison to reference analgesics following cisplatin treatment. *Pharmacol Res.* 2013; 67:94–109. [PubMed: 23127915]
- Gulyas AI, Cravatt BF, Bracey MH, Dinh TP, Pomelli D, Boscia F, Freund TF. Segregation of two endocannabinoid-hydrolyzing enzymes into pre- and postsynaptic compartments in the rat hippocampus, cerebellum and amygdala. *Eur J Neurosci.* 2004; 20:441–458. [PubMed: 15233753]
- Håjos N, Katona I, Naiem SS, Mackie K, Ledent C, Mody I, Freund TF. Cannabinoids inhibit hippocampal and network oscillations. *Eur J Neurosci.* 2000; 12:3239–3249. [PubMed: 10998107]
- Hermanson DJ, Gamble-George JC, Marnett LJ, Patel S. Substrate-selective COX-2 inhibition as a novel strategy for therapeutic endocannabinoid augmentation. *Trends Pharmacol Sci.* 2014; 35:358–367. [PubMed: 24845457]
- Hernández-Torres G, Cipriano M, Hedén E, Björklund E, Canales Á, Zian D, Feliú A, Mecha M, Guaza C, Fowler CJ, Ortega-Gutiérrez S, López-Rodríguez ML. A reversible and selective inhibitor of monoacylglycerol lipase ameliorates multiple sclerosis. *Angew Chem Int Ed Engl.* 2014; 53:13765–13770. [PubMed: 25298214]
- Higgins A, Yuan S, Wang Y, Burrell BD. Differential modulation of nociceptive versus non-nociceptive synapses by endocannabinoids. *Mol Pain.* 2013; 1(9):26. [PubMed: 23725095]
- Hohmann AG, Suplita RL, Bolton NM, Neely MH, Fegley D, Mangieri R, Krey JF, Walker JM, Holmes PV, Crystal JD, Duranti A, Tontini A, Mor M, Tarzia G, Piomelli D. An endocannabinoid mechanism for stress-induced analgesia. *Nature.* 2005; 435:1108–1112. [PubMed: 15973410]
- Hornaaert, C. Triazolopyridine carboxamides derivatives, preparation thereof, and therapeutic uses thereof. Patent US7868007B2. 2011.
- Hu SS, Bradshaw HB, Chen JS, Tan B, Walker JM. Prostaglandin E2 glycerol ester, an endogenous COX-2 metabolite of 2-arachidonoylglycerol, induces hyperalgesia and modulates NF κ B activity. *Br J Pharmacol.* 2008; 153:1538–1549. [PubMed: 18297109]
- Izumi Y, Zorumski CF. NMDA receptors, mGluR5, and endocannabinoids are involved in a cascade leading to hippocampal long-term depression. *Neuropsychopharmacology.* 2012; 37:609–617. [PubMed: 21993209]
- Jhaveri MD, Richardson D, Robinson I, Garle MJ, Patel A, Sun Y, Sagar DR, Bennett AJ, Alexander SP, Kendall DA, Chapman V. Inhibition of fatty acid amide hydrolase and cyclooxygenase-2 increases levels of endocannabinoid related molecules and produces analgesia via peroxisome proliferator-activated receptor-alpha in a model of inflammatory pain. *Neuropharmacology.* 2008; 55:85–93. [PubMed: 18534634]
- Kapanda CN, Muccioli GG, Labar G, Poupaert JH, Lambert DM. Bis(dialkylaminethiocarbonyl)disulfides as potent and selective monoglyceride lipase inhibitors. *J Med Chem.* 2009; 52:7310–7314. [PubMed: 19883085]
- Karlsson M, Contreras JA, Hellman U, Tornqvist H, Holm C. cDNA cloning, tissue distribution, and identification of the catalytic triad of monoglyceride lipase. *J Biol Chem.* 1997; 272:27218–27223. [PubMed: 9341166]
- Käsänen H, Minkkilä A, Taupila S, Patel JZ, Parkkari T, Lahtela-Kakkonen M, Saario SM, Nevalainen T, Poso A. 1,3,4-Oxadiazol-2-ones as fatty-acid amide hydrolase and monoacylglycerol lipase inhibitors: Synthesis, in vitro evaluation and insight into potency and selectivity determinants by molecular modelling. *Eur J Pharm Sci.* 2013; 49:423–433. [PubMed: 23557840]

- Kathuria S, Gaetani S, Fegley D, Valiño F, Duranti A, Tontini A, Mor M, Tarzia G, La Rana G, Calignano A, Giustino A, Tattoli M, Palmery M, Cuomo V, Piomelli D. Modulation of anxiety through blockade of anandamide hydrolysis. *Nat Med.* 2003; 9:76–81. [PubMed: 12461523]
- Kim J, Alger BE. Inhibition of cyclooxygenase-2 potentiates retrograde endocannabinoid effects in hippocampus. *Nature Neurosci.* 2004; 7:697–698. [PubMed: 15184902]
- King AR, Duranti A, Tontini A, Rivara S, Rosengarth A, Clapper JR, Astarita G, Geaga JA, Luecke H, Mor M, Tarzia G, Piomelli D. URB602 inhibits monoacylglycerol lipase and selectively blocks 2-arachidonoylglycerol degradation in intact brain slices. *Chem Biol.* 2007; 14:1357–1365. [PubMed: 18096504]
- King AR, Lodola A, Carmi C, Fu J, Mor M, Piomelli D. A critical cysteine residue in monoacylglycerol lipase is targeted by a new class of isothiazolinone-based enzyme inhibitors. *Br J Pharmacol.* 2009a; 157:974–983. [PubMed: 19486005]
- King AR, Dotsey EY, Lodola A, Jung KM, Ghomian A, Qiu Y, Fu J, Mor M, Piomelli D. Discovery of potent and reversible monoacylglycerol lipase inhibitors. *Chem Biol.* 2009b; 16:1045–1052. [PubMed: 19875078]
- Kinsey SG, Wise LE, Ramesh D, Abdullah R, Selley DE, Cravatt BF, Lichtman AH. Repeated low-dose administration of the monoacylglycerol lipase inhibitor JZL184 retains cannabinoid receptor type 1-mediated antinociceptive and gastroprotective effects. *J Pharmacol Exp Ther.* 2013; 345:492–501. [PubMed: 23412396]
- Kozak KR, Prusakiewicz JJ, Rowlinson SW, Schneider C, Marnett LJ. Amino acid determinants in cyclooxygenase-2 oxygenation of the endocannabinoid 2-arachidonoylglycerol. *J Biol Chem.* 2001; 276:30072–30077. [PubMed: 11402053]
- Kozak KR, Rowlinson SW, Marnett LJ. Oxygenation of the endocannabinoid, 2-arachidonoylglycerol, to glyceryl prostaglandins by cyclooxygenase-2. *J Biol Chem.* 2000; 275:33744–33749. [PubMed: 10931854]
- Kreutz S, Koch M, Böttger C, Ghadban C, Korf HW, Dehghani F. 2-Arachidonoylglycerol elicits neuroprotective effects on excitotoxically lesioned dentate gyrus granule cells via abnormal-cannabidiol-sensitive receptors on microglial cells. *Glia.* 2009; 57:286–294. [PubMed: 18837048]
- Labar G, Bauvois C, Muccioli GG, Wouters J, Lambert DM. Disulfiram is an inhibitor of human purified monoacylglycerol lipase, the enzyme regulating 2-arachidonoylglycerol signaling. *Chem Bio Chem.* 2007; 8:1293–1297.
- Labar G, Bauvois C, Borel F, Ferrer JL, Wouters J, Lambert DM. Crystal structure of the human monoacylglycerol lipase, a key actor in endocannabinoid signaling. *Chem Bio Chem.* 2010; 11:218–227.
- Laitinen T, Navia-Paldanius D, Ryttilahti R, Marjamaa JJT, Ka ízková J, Parkkari T, Pantsar T, Poso A, Laitinen JT, Savinainen JR. Mutation of Cys242 of human monoacylglycerol lipase disrupts balanced hydrolysis of 1- and 2-monoacylglycerols and selectively impairs inhibitor potency. *Mol Pharmacol.* 2013; 85:510–519. [PubMed: 24368842]
- Lichtman AH, Hawkins EG, Griffin G, Cravatt BF. Pharmacological activity of fatty acid amides is regulated, but not mediated, by fatty acid amide hydrolase in vivo. *J Pharmacol Exp Ther.* 2002; 302:73–79. [PubMed: 12065702]
- Long JZ, Li W, Booker L, Burston JJ, Kinsey SG, Schlosburg JE, Pavón FJ, Serrano AM, Selley DE, Parson LH, Lichtman AH, Cravatt BF. Selective blockade of 2-arachidonoylglycerol hydrolysis produces cannabinoid behavioral effects. *Nat Chem Biol.* 2009a; 5:37–44. [PubMed: 19029917]
- Long JZ, Nomura DK, Cravatt BF. Characterization of monoacylglycerol lipase inhibition reveals differences in central and peripheral endocannabinoid metabolism. *Chem Biol.* 2009b; 16:744–753. [PubMed: 19635411]
- Long JZ, Nomura DK, Vann RE, Walentiny DM, Booker L, Jin X, Burston JJ, Sim-Selley LJ, Lichtman AH, Wiley JL, Cravatt BF. Dual blockade of FAAH and MAGL identifies behavioral processes regulated by endocannabinoid crosstalk in vivo. *Proc Natl Acad Sci U S A.* 2009; 106:20270–20275. [PubMed: 19918051]
- Lysenko LV, Kim J, Henry C, Tyrtysnaia A, Kohnz RA, Madamba F, Simon GM, Kleschenvnikova NE, Nomura DK, Ezekowitz RAB, Kleschenvnikov AM. Monoacylglycerol lipase inhibitor JZL184

- improves behavior and neural properties in Ts65Dn mice, a model of down syndrome. *Plos ONE*. 2014; 9(12):e114521. [PubMed: 25474204]
- Marrs WR, Blankman JL, Horne EA, ThomazEAU A, Lin YH, Coy J, Bodor AL, Muccioli GG, Hu SS, Woodruff G, Fung S, Lafourcade M, Alexander JP, Long JZ, Li W, Xu C, Möller T, Mackie K, Manzoni OJ, Cravatt BF, Stella N. The serine hydrolase ABHD6 controls the accumulation and efficacy of 2-AG at cannabinoid receptors. *Nat Neurosci*. 2010; 13:951–957. [PubMed: 20657592]
- Matuszak N, Muccioli GG, Labar G, Lambert DM. Synthesis and in vivo evaluation of N-substituted maleimide derivatives as selective monoglyceride lipase inhibitors. *J Med Chem*. 2009; 52:7410–7420. [PubMed: 19583260]
- Matuszak N, Es Saadi B, Labar G, Marchan-Brynaert J, Lambert DM. Benzisothiazolinone as a useful template for the design of new monoacylglycerol lipase inhibitors: Investigation of the target residues and comparison with octhilinone. *Bioorg Med Chem Lett*. 2011; 21:7321–7324. [PubMed: 22056744]
- Mechoulam R, Ben-Shabat S, Hanus L, Ligumsky M, Kaminski NE, Schatz AR, Gopher A, Almog S, Martin BR, Compton DR, Pertwee RG, Griffin G, Bayewitch M, Barg J, Vogel Z. Identification of an endogenous 2-monoglyceride, present in canine gut, that binds to cannabinoid receptors. *Biochem Pharmacol*. 1995; 50:83–90. [PubMed: 7605349]
- Muccioli GG, Xu C, Odah E, Cudaback E, Cisneros JA, Lambert DM, López Rodríguez ML, Bajjalieh S, Stella N. Identification of a novel endocannabinoid-hydrolyzing enzyme expressed by microglial cells. *J Neurosci*. 2007; 27:2883–2889. [PubMed: 17360910]
- Niphakis MJ, Cognetta AB 3rd, Chang JW, Buczynski MW, Parsons LH, Byrne F, Burston JJ, Chapman V, Cravatt BF. Evaluation of NHS carbamates as a potent and selective class of endocannabinoid hydrolase inhibitors. *ACS Chem Neurosci*. 2013; 4:1322–1332. [PubMed: 23731016]
- Nomura DK, Long JZ, Niessen S, Hoover HH, Ng S, Cravatt BF. Monoacylglycerol lipase regulates a fatty acid network that promotes cancer pathogenesis. *Cell*. 2010; 140:49–61. [PubMed: 20079333]
- Nomura DK, Morrison BE, Blankman JL, Long JZ, Kinsey SG, Marcondes MCG, Ward AM, Hahn YK, Lichtman AH, Conti B, Cravatt BF. Endocannabinoid hydrolysis generates brain prostaglandins that promote neuroinflammation. *Science*. 2011; 334:809–813. [PubMed: 22021672]
- Nomura DK, Lombardi DP, Chang JW, Niessen S, Ward AM, Long JZ, Hoover HH, Cravatt BF. Monoacylglycerol lipase exerts dual control over the endocannabinoid and fatty acid pathways to support prostate cancer. *Chem Biol*. 2011; 18:846–856. [PubMed: 21802006]
- Ortar G, Morera E, De Petrocellis L, Ligresti A, Schiano Moriello A, Morera L, Nalli M, Ragno R, Pirolli A, Di Marzo V. Biaryl tetrazolyl ureas as inhibitors of endocannabinoid metabolism: modulation at the N-portion and distal phenyl ring. *Eur J Med Chem*. 2013; 63:118–132. [PubMed: 23474898]
- Oudin MJ, Gajendra S, Williams G, Hobbs C, Lalli G, Doherty P. Endocannabinoids regulate the migration of subventricular zone-derived neuroblast in the postnatal brain. *J Neurosci*. 2011; 31:4000–4011. [PubMed: 21411643]
- Pasquarelli N, Porazik C, Hanselmann J, Weydt P, Ferger B, Witting A. Comparative biochemical characterization of the monoacylglycerol lipase inhibitor KML29 in brain, spinal cord, liver, spleen, fat and muscle tissue. *Neuropharmacology*. 2015; 91:148–156. [PubMed: 25497453]
- Piro JR, Benjamin DI, Duerr JM, Pi Y, Gonzales C, Wood KM, Schwartz JW, Nomura DK, Samad TA. A dysregulated endocannabinoid-icosanoid network supports pathogenesis in a mouse model of Alzheimer's disease. *Cell Rep*. 2012; 1:617–623. [PubMed: 22813736]
- Puente N, Cui Y, Lassalle O, Lafourcade M, Georges F, Venance L, Grandes P, Manzoni OJ. *Nat Neurosci*. 2011; 14:1542–1547. [PubMed: 22057189]
- Piomelli D, Astarita G, Rapaka R. A neuroscientist's guide to lipidomics. *Nat Rev Neurosci*. 2007; 8:743–754. [PubMed: 17882252]
- Piomelli D. More surprises lying ahead. The endocannabinoids keep us guessing. *Neuropharmacology*. 2014; 76:228–234. [PubMed: 23954677]

- Reis P, Holmberg K, Watzke H, Leser ME, Miller R. Lipases at interfaces: a review. *Adv Colloid Interface Sci.* 2009; 147–148:237–250.
- Saario SM, Salo OMH, Nevalainen T, Poso A, Laitinen JT, Järvinen T, Niemi R. Characterization of the sulfhydryl-sensitive site in the enzyme responsible for hydrolysis of 2-arachidonoyl-glycerol in rat cerebellar membranes. *Chem Biol.* 2005; 12:649–656. [PubMed: 15975510]
- Schalk-Hihi C, Schubert C, Alexander R, Bayouny S, Clemente JC, Deckman I, DesJarlais R, Dzordzorme KC, Flores CM, Grasberger B, Kranz JK, Lewandowski F, Liu L, Ma H, Maguire D, Macielag MJ, McDonnell ME, Mezzasalma Haarlander T, Miller R, Milligan C, Reynolds C, Kuo LC. Crystal structure of a soluble form of human monoglyceride lipase in complex with an inhibitor at 1.35 Å resolution. *Protein Sci.* 2011; 20:670–683. [PubMed: 21308848]
- Schlosburg JE, Blankman JL, Long JZ, Nomura DK, Pan B, Kinsey SG, Nguyen PT, Ramesh D, Booker L, Burston JJ, Thomas EA, Selley DE, Sim-Selley LJ, Liu Q, Lichtman AH, Cravatt BF. Chronic monoacylglycerol lipase blockade causes functional antagonism of the endocannabinoid system. *Nat Neurosci.* 2010; 13:1113–1119. [PubMed: 20729846]
- Shonesy BC, Bluett RJ, Ramikie TS, Baldi R, Hermanson DJ, Kingsley PJ, Marnett LJ, Winder DG, Colbran RJ, Patel S. Genetic disruption of 2-arachidonoylglycerol synthesis reveals a key role for endocannabinoid signaling in anxiety modulation. *Cell Rep.* 2014; 9:1644–1653. [PubMed: 25466252]
- Sciolino NR, Zhou W, Hohmann AG. Enhancement of endocannabinoid signaling with JZL184, an inhibitor of the 2-arachidonoylglycerol hydrolyzing enzyme monoacylglycerol lipase, produces anxiolytic effects under conditions of high environmental aversiveness in rats. *Pharmacol Res.* 2011; 64:226–234. [PubMed: 21600985]
- Stella N, Schweitzer P, Piomelli D. A second endogenous cannabinoid that modulates long-term potentiation. *Nature.* 1997; 388:773–777. [PubMed: 9285589]
- Sugiura T, Kondo S, Sukagawa A, Nakane S, Shinoda A, Itoh K, Yamashita A, Waku K. 2-Arachidonoylglycerol: a possible endogenous cannabinoid receptor ligand in brain. *Biochem Biophys Res Commun.* 1995; 215:89–97. [PubMed: 7575630]
- Szabo M, Agostino M, Malone DT, Yuriev E, Capuano B. The design, synthesis and biological evaluation of novel URB602 analogues as potential monoacylglycerol lipase inhibitors. *Bioorg Med Chem Lett.* 2011; 21:6782–6787. [PubMed: 21982493]
- Tornqvist H, Belfrage P. Purification and some properties of a monoacylglycerol-hydrolyzing enzyme of rat adipose tissue. *J Biol Chem.* 1976; 251:813–819. [PubMed: 1249056]
- Tuccinardi T, Granchi C, Rizzolio F, Caligiuri I, Battistello V, Toffoli G, Minutolo F, Macchia M, Martinelli A. Identification and characterization of a new reversible MAGL inhibitor. *Bioorg Med Chem.* 2014; 22:3285–3291. [PubMed: 24853323]
- Ueda N, Tsuboi K, Uyama T. Metabolism of endocannabinoids and related N-acyl ethanolamines: Canonical and alternative pathways. *FEBS Journal.* 2013; 280:1874–1894. [PubMed: 23425575]
- Valdeolivas S, Pazos MR, Bisogno T, Piscitelli F, Iannotti FA, Allarà M, Sagredo O, Di Marzo V, Fernández-Ruiz J. The inhibition of 2-arachidonoyl-glycerol (2-AG) biosynthesis, rather than enhancing striatal damage, protects striatal neurons from malonate-induced death: a potential role of cyclooxygenase-2-dependent metabolism of 2-AG. *Cell Death Dis.* 2013; 17(4):e862. [PubMed: 24136226]
- Xu YJ, Chen C. Endocannabinoids in synaptic plasticity and neuroprotection. *Neuroscientist.* 2015; 21(2):152–168. [PubMed: 24571856]
- Ye L, Zhang B, Seviour EG, Tao K, Liu X, Ling Y, Chen J, Wang G. Monoacylglycerol lipase (MAGL) knockdown inhibits tumor cells growth in colorectal cancer. *Cancer Lett.* 2011; 307:6–17. [PubMed: 21543155]
- Zhang J, Hu M, Teng Z, Tang YP, Chen C. Synaptic and cognitive improvements by inhibition of 2-AG metabolism are through upregulation of microRNA-188-3p in a mouse model of Alzheimer's disease. *J Neurosci.* 2014; 34:14919–14933. [PubMed: 25378159]
- Zvonok N, Williams J, Johnston M, Pandarinathan L, Janero DR, Li J, Krishnan SC, Makriyannis A. Full mass spectrometric characterization of human monoacylglycerol lipase generated by large-scale expression and single-step purification. *J Proteome Res.* 2008a; 7:2158–2164. [PubMed: 18452279]

Zvonok N, Pandarinathan L, Williams J, Johnston M, Karageorgos I, Janero DR, Krishnan SC, Makryiannis A. Covalent inhibitors of human monoacylglycerol lipase: ligand-assisted characterization of the catalytic site by mass spectrometry and mutational analysis. *Chem Biol.* 2008b; 15:854–862. [PubMed: 18721756]

Author Manuscript

Author Manuscript

Author Manuscript

Author Manuscript

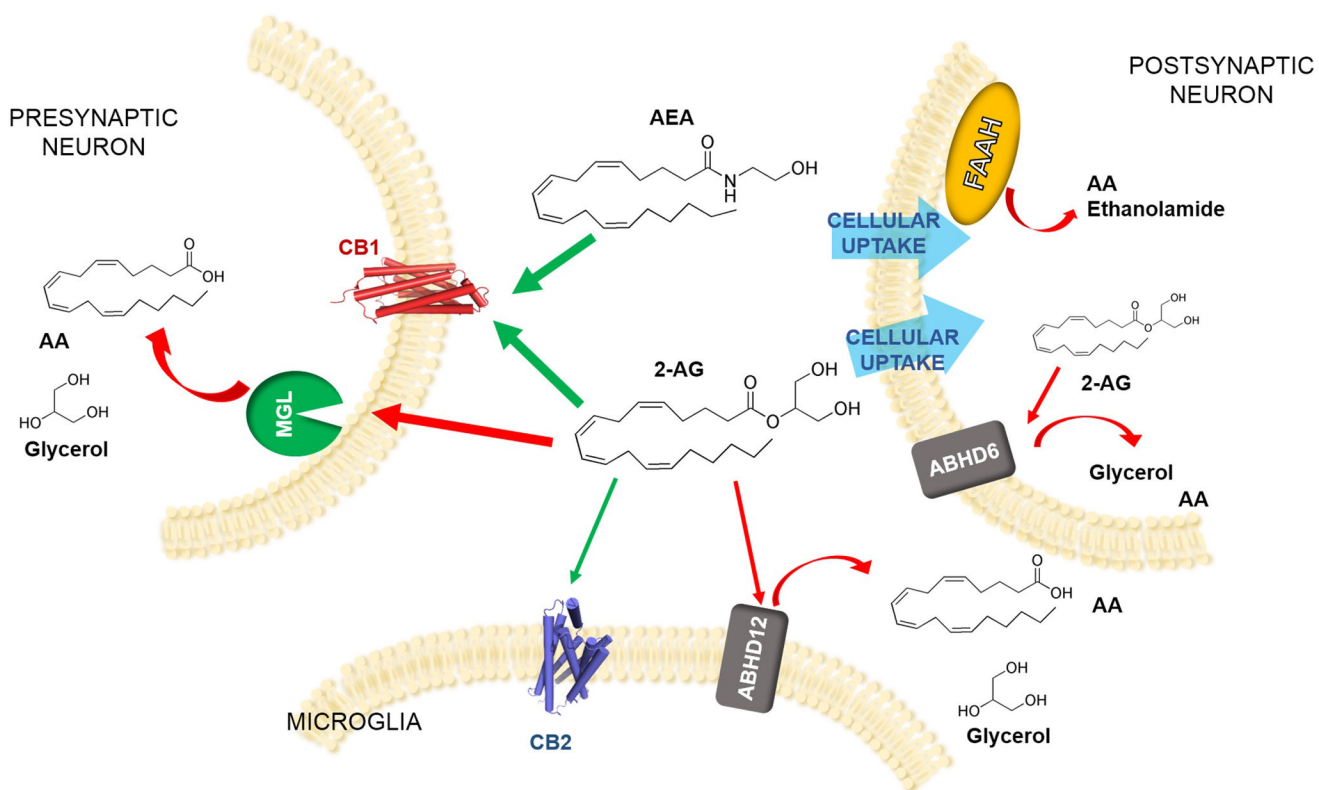


Figure 1.
Schematic overview of 2-AG metabolism.

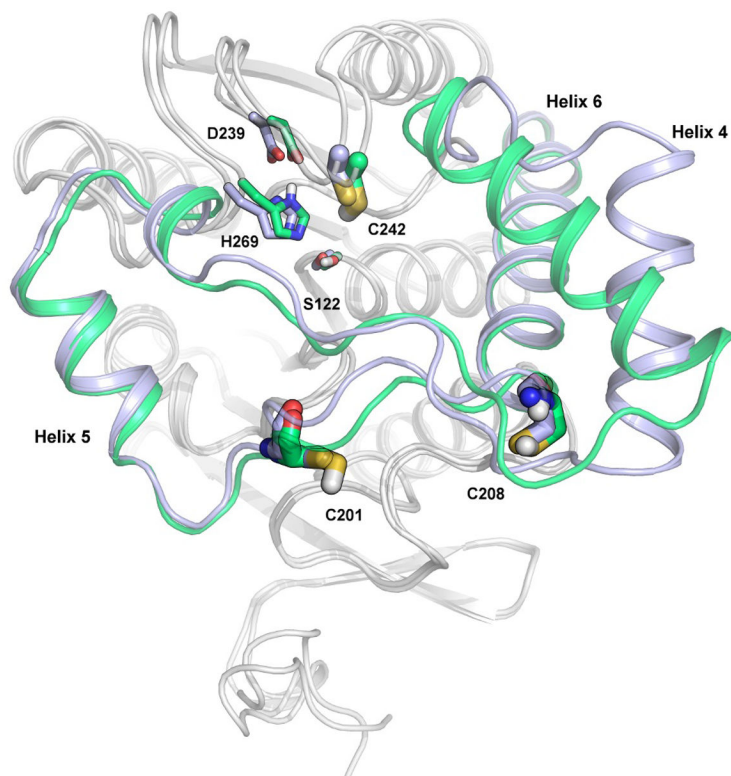


Figure 2. Superposition of MGL-crystallized structures with regulatory cysteines (Cys201, Cys208 and Cys242) shown as bold sticks. The catalytic triad residues are shown as sticks. The crystal structures present different conformations of the lid domain. The lid domain in its open conformation (PDB: 3HJU) is colored in light blue; the lid domain in closed conformation (PDB: 3PE6) is colored in green.

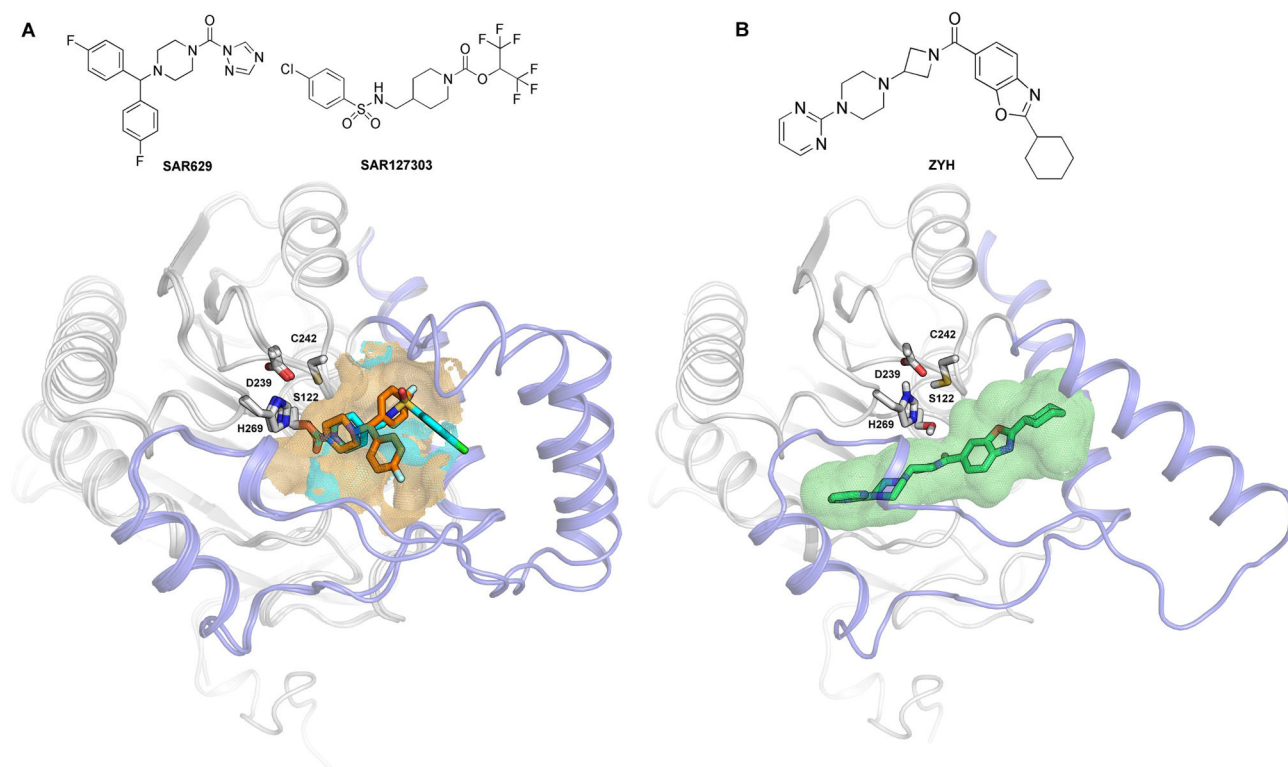


Figure 3. Crystallized MGL-inhibitor complexes. Panel A: superposition of MGL crystal structures (represented with grey cartoon; the lid domain is blue-colored; side chains of the catalytic triad and of Cys242 are represented in sticks with grey carbons) covalently bound to the irreversible inhibitors SAR629 (PDB: 3JWE, orange carbons) and SAR127303 (PDB: 4UUQ, cyan carbons). Panel B: crystal structure of MGL (PDB: 3PE6) in complex with the inhibitor ZYH (green carbons).

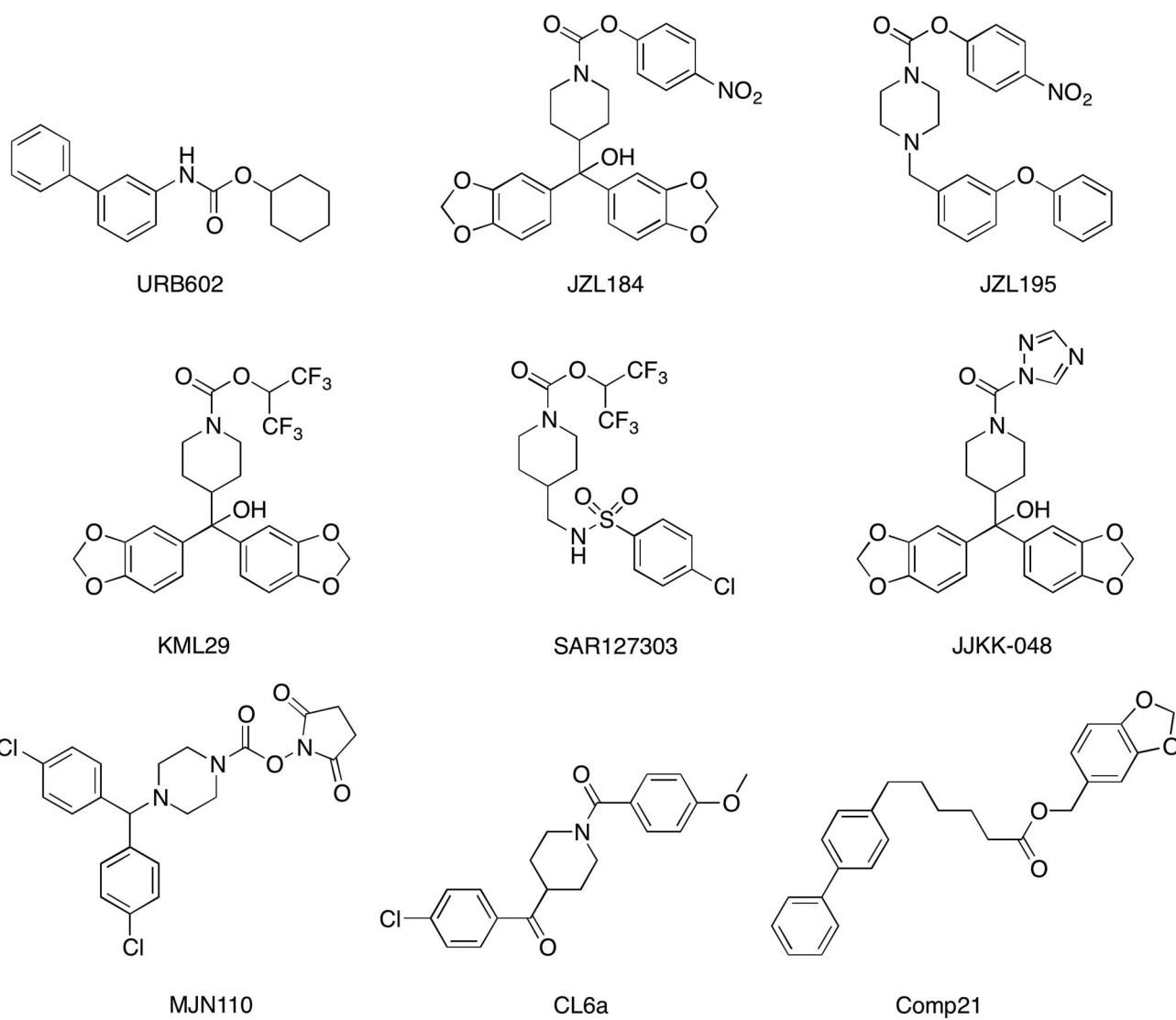
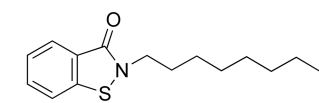
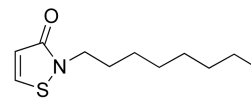


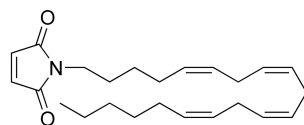
Figure 4.
Structures of MGL inhibitors targeting the catalytic pocket.



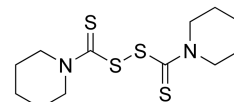
N-octylbenzothiazolinone



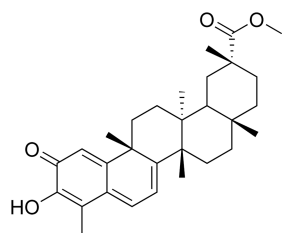
Octhilinone



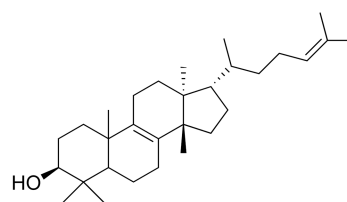
NAM



Dicyclopentamethylenethiuram disulfide



Pristimerin



Euphol

Figure 5.
Structures of MGL inhibitors that interact with regulatory cysteines.